

## Observation of scalar longitudinal electrodynamic waves

C. MONSTEIN<sup>1</sup> and J. P. WESLEY<sup>2</sup>

<sup>1</sup> *ETHZ, Institute of Astronomy - Scheuchzerstrasse 7, CH-8092 Zürich, Switzerland*

<sup>2</sup> *Weiherdammstrasse 24, D-78176 Blumberg, Germany*

(received 18 February 2002; accepted in final form 14 May 2002)

PACS. 41.20.-q – Applied classical electromagnetism.

PACS. 41.20.Jb – Electromagnetic wave propagation; radiowave propagation.

**Abstract.** – Theoretically scalar potential  $\Phi$  waves with a longitudinal electric field  $\vec{E}$  in the direction of propagation must exist. A centrally fed ball antenna, 6 cm diameter, producing a pulsating 433.59 MHz spherical source charge, generated such a wave, that was detected by an identical ball antenna. The longitudinality of  $\vec{E}$  was demonstrated by intervening a cubic array of 9 half-wavelength wires, that absorbed the wave when the wires were parallel (but not when perpendicular) to the direction of propagation. The signal from the ball antenna source, placed 4.0 m above ground and receiver 4.4 m above ground, was measured as a function of distance, yielding satisfactory agreement with theory, including 2 expected interference minima produced by an image source induced in the Earth. Only waves can yield such an interference and can be reflected from the Earth's surface and vary as the inverse square of distance.

*Theory.* – From Coulomb's law, the scalar potential  $\Phi$  is a solution to Laplace's equation. Introducing time retardation,  $\Phi$  becomes a solution to the inhomogeneous wave equation [1–3],

$$\nabla^2\Phi - \partial^2\Phi^2/\partial t^2c^2 = -4\pi\rho, \quad (1)$$

where  $\rho$  is the source charge density. Solutions to this wave equation (1) are scalar waves, where the energy flux  $\vec{S}$  and density  $D$  are given by

$$\vec{S} = -\nabla\Phi \partial\Phi/\partial t, \quad D = (\nabla\Phi)^2/2 + (\partial\Phi/\partial t)^2/2. \quad (2)$$

A spherical surface with a uniform periodic changing net charge  $q$  is equivalent to a pulsating point charge density at  $\vec{r}'$  given by

$$\rho = q\delta(\vec{r} - \vec{r}') \sin(\omega t). \quad (3)$$

The solution to the wave equation (1) with the source charge density given by eq. (3) is for  $\vec{r}' = 0$

$$\Phi = q \sin(kr - \omega t)/r, \quad (4)$$

where  $k = 2\pi/\lambda$  is the propagation constant and  $\omega = 2\pi f$  is the angular frequency. Here,  $\lambda$  stands for wavelength, where  $\lambda = c/f$ , whereby  $f$  is the frequency of the transmitted signal

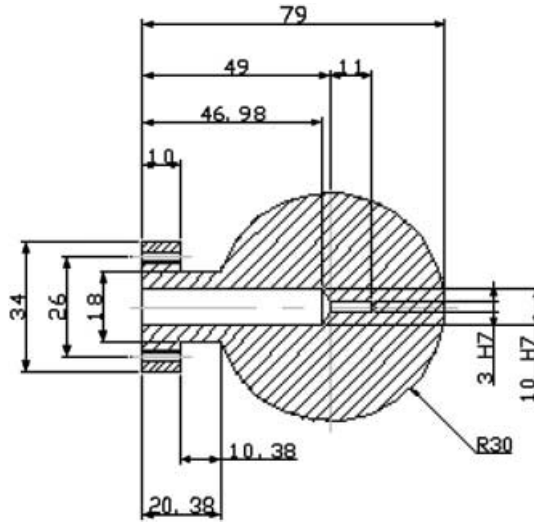


Fig. 1 – Sketch of the aluminium ball antennas. All given dimensions are in mm.

and  $c$  is the speed of light in vacuum. The spherically symmetric radiating longitudinal electric field is then

$$\vec{E} = \nabla\Phi = [k q \cos(kr - \omega t)/r - q \sin(kr - \omega t)/r^2]\vec{e}_r, \quad (5)$$

where  $\vec{e}_r$  is a unit vector in the radial direction. The time average flux from eq. (4) and the first of equations (2) is

$$\langle \vec{S} \rangle_t = k \omega q / (2r^2) \vec{e}_r, \quad (6)$$

where  $\langle \rangle_t$  denotes temporal average. Thus, the elementary theory, compatible with Maxwell theory, yields the necessary conclusion that scalar  $\Phi$ , or longitudinal  $\vec{E}$ , or Coulomb electrodynamic waves must exist. The usual assumption that such waves cannot exist has no theoretical justification.

*The ball antenna source.* – The geometry of the spherical antenna is indicated in fig. 1. A 433.59 MHz signal is fed into the inside of the metal sphere through a coaxial cable, where the outside grounded conductor acts as a shield. The result is an oscillating uniform spherical charge density that is the source of the radiating longitudinal electric  $\vec{E}$  field. Mathematically a spherically symmetric source can generate only scalar waves; so the ball antenna can only generate a  $\Phi$ -wave, and, thus, only a longitudinal electrodynamic  $\vec{E}$ -wave. The spherically symmetric current density  $\vec{J}$  within the ball, that gives rise to the pulsating surface charge source, is divergenceless,  $\nabla \cdot \vec{J} = 0$ ; so  $\nabla \cdot \vec{A} = 0$  and  $\nabla \times \vec{A} = 0$ ; and no transverse wave can arise. The ball antenna as a receiver detects the net charge induced by the component of the incident  $\vec{E}$  field normal to the front surface; so only longitudinal  $\vec{E}$ -waves can be detected. An absorbing screen can be introduced to determine the direction of the incident longitudinal wave. Stray transverse fields generated by leads and neighboring objects play only a minor role.

*Longitudinal electrodynamic waves transport the energy across a parallel plate condenser.* – It is well known that energy can be transmitted from one plate of a parallel plate condenser to the other. Thus, it is trivially obvious that energy is transmitted in the direction of an electric  $\vec{E}$  field across the condenser. Since normally the plates are much closer than a wavelength

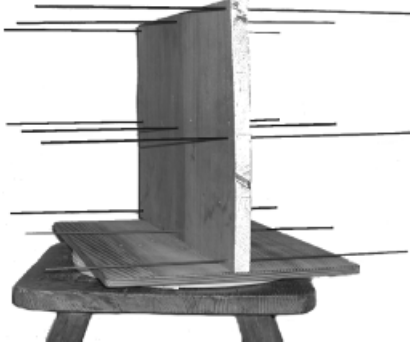


Fig. 2

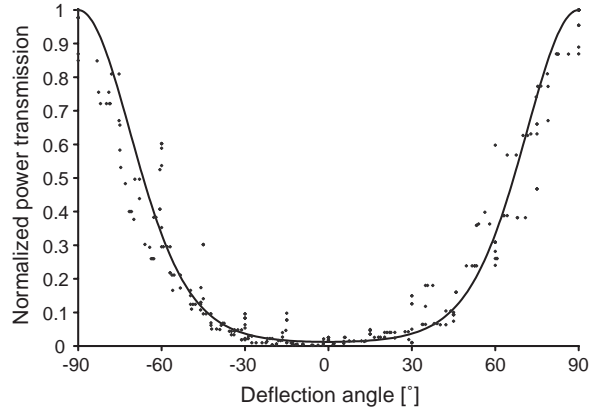


Fig. 3

Fig. 2 – Rotatable  $3 \times 3$  polarizer on top of a wooden chair with  $\lambda/2$  rods made of brass. The polarizer can either be turned by hand or by the help of a disc record player.

Fig. 3 – The measured transmission coefficient  $T$  (shown as points) for longitudinal waves at 433.59 MHz passing through the polarizer-analyzer (shown in fig. 2) as a function of the polarizer angle  $\phi$  between the direction of the wires and the direction of propagation. The solid curve presents the theory, eq. (9),  $T = \exp[-4.4 \cos^2(\phi)]$  for the best-fit value of  $\kappa$ .

apart, this is usually assumed to be no proof of longitudinal electrodynamic waves. Yet the theory presented above is quite independent of the size of the wavelength; so the flow of energy across an ordinary condenser does, in fact, demonstrate the existence of longitudinal electrodynamic waves. One of us (Monstein) extended the distance between two parallel plates of a parallel plate condenser from near to more than a wavelength and continued to register a flow of energy from one plate to the other, as expected from the theory for longitudinal electrodynamic waves.

*Demonstration of the longitudinality of the observed waves.* – Figure 2 shows a cubic array of 9 wires of length  $\lambda/2$  (34.6 cm) that was employed as a polarizer-analyzer for longitudinal waves. If the wires are oriented parallel to the  $\vec{E}$  field in the direction of propagation, the signal is reduced, as indicated in fig. 3. If the wires are oriented perpendicular to the  $\vec{E}$  field, the signal transmitted through the array is a maximum. Two such arrays with wires perpendicular to the direction of propagation and to each other serve as a filter to absorb transverse waves of any polarization, while transmitting longitudinal waves. The fractional energy flux, or the transmission coefficient  $T$ , for the longitudinal waves through the polarizer-analyzer as a function of the angle  $\phi$  between the direction of the wires and the direction of propagation may be determined by noting that only the  $\vec{E}$  field component  $E_0 \cos(\phi)$  in the direction of a wire produces Ohmic losses. The Ohmic loss  $\delta P$  per unit time in an element  $\delta L$  of the wire is then equal to  $\delta P = -(\delta V)^2/\delta R$ , where  $\delta V = E_0 \cos(\phi)\delta L$  is the potential across the element  $\delta L$  and where  $\delta R = \delta L/\sigma A$  is the resistance of the wire element of length  $\delta L$ , and  $A$  is the cross-sectional area and  $\sigma$  the conductivity of the brass wires; thus,

$$\delta P = -[\sigma A E_0^2 \cos^2(\phi)] \delta L. \quad (7)$$

It may be readily shown from the first of eqs. (2) that the time average energy flux in the wire equals the time average electric field  $E_0$  squared times  $c$ ,  $\langle P/A \rangle_t = \langle S \rangle_t = cE_0^2$ . Thus, from

eq. (7) for the rate of energy flow loss  $\delta\langle S \rangle_t$  in the wire per unit length  $\delta L$  is given by

$$\delta\langle S \rangle_t = -(\sigma/c) \cos^2(\phi) \langle S \rangle_t \delta L. \quad (8)$$

Integrating eq. (8), the fractional energy transmitted through the wire of length  $L$  is

$$T = \exp[-\kappa \cos^2(\phi)], \quad (9)$$

where  $\kappa$  is a constant proportional to the length  $L$  of the wire. The fractional energy transmitted, the transmission coefficient  $T$ , for the longitudinal waves passing between the 9 wires in the polarizer-analyzer should have precisely the same dependence on  $\phi$ . Thus, the theoretical result eq. (9) can be chosen to fit the observations when  $\kappa = 4.4$ , as shown in fig. 3. Since transverse electrodynamic waves with the  $\vec{E}$  vector perpendicular to both the wires and to the direction of propagation would pass unhampered through the polarizer-analyzer, the observed absorption of the signal for  $\phi = 0$  is clear evidence that a longitudinal wave is involved and not a transverse wave. This then demonstrates that longitudinal electrodynamic waves can, and do, exist.

*Theory for the signal as a function of distance.* – The source ball antenna was placed a distance  $y$  above ground; and the detector ball antenna was placed a distance  $y'$  above ground and at a distance  $x$  from the source, as shown in fig. 4. It is clear that the conducting Earth will produce an image of the source; so the observed signal is a superposition of two spherical waves, one of amplitude  $A$  from the source at  $y$  and the other of amplitude  $B$  from the image at  $-y$  as observed at the point  $x, y'$ . The potential field  $\Phi$  at the point of observation, using eq. (4), then becomes

$$\Phi = A \sin(kR - \omega t)/R + B \sin(kR' - \omega t)/R', \quad (10)$$

where

$$R^2 = (y' - y)^2 + x^2, \quad R'^2 = (y' + y)^2 + x^2. \quad (11)$$

Since the conductivity of the Earth is only about  $10^{-3}$  U/m [4], the effective reflecting surface of the Earth is a little below the actual surface. To agree with observations, the effective surface is chosen as half wavelength,  $\lambda/2 = 34.6$  cm, below the actual surface. The values of the effective heights of the ball antennas are then

$$y = 4.346 \text{ m} \quad \text{and} \quad y' = 4.746 \text{ m}. \quad (12)$$

The signal observed equals the time average energy flux  $\vec{S}$ , as given by the first of eqs. (2). Only the  $x$ -component of  $\vec{S}$  need be considered; as  $y$  and  $y'$  are small compared to all distances  $x > 10$  m. Substituting eqs. (10) and (11) into the first of eqs. (2) and taking time averages yields, after a rather lengthy but straightforward analysis,

$$\begin{aligned} \langle S_x \rangle_t = & (\omega k x / 2 R^3 R'^3) [B^2 R^3 + A^2 R'^3 + A B R R' (R + R') \cos k(R' - R) + \\ & + (A B / k) (R^2 - R'^2) \sin k(R' - R)]. \end{aligned} \quad (13)$$

For the present experiment the last term in the brackets may be neglected, as it varies relative to the third term in the brackets as  $\lambda y y' / \pi x < 5 \cdot 10^{-3}$  for  $x > 10$  m. The expression to be compared with the observations becomes then

$$\langle S_x \rangle_t = (\omega k x / 2 R^3 R'^3) [B^2 R^3 + A^2 R'^3 + A B R R' (R + R') \cos k(R' - R)]. \quad (14)$$

TABLE I – *Position of wave minima as a function of radial distance  $x$  (m).*

$n$	$x_{\min}$
0	119
1	39
2	23
3	16

A simple asymptotic approximation for large  $x$ , illustrating most of the theoretical features of the signal, is obtained by replacing  $R$  and  $R'$  by  $x$  (thus, neglecting  $y$  and  $y'$ ), except for the difference ( $R' - R$ ) necessary to give the sinusoidal variation; thus,

$$\langle S_x \rangle_t \sim (\omega k/2x^2)[A^2 + B^2 + 2AB \cos k(R' - R)]. \quad (15)$$

For  $x$  very large the cosine term becomes unity, which then yields

$$\langle S_x \rangle_t \sim (\omega k/2x^2)(A + B)^2, \quad (16)$$

which reveals the variation with the inverse square of the distance, as it should for a wave. The minima are given for

$$R' - R = (2n + 1)\lambda/2, \quad (17)$$

where  $n$  is an integer. Substituting in the expressions for  $R$  and  $R'$ , eqs. (11), and solving for  $x$  yields

$$x_{\min}^2 = -y^2 - y'^2 + 16y^2y'^2/(2n + 1)^2\lambda^2 + (2n + 1)^2\lambda^2/16. \quad (18)$$

Introducing the values of  $y$  and  $y'$ , as given by eq. (12), into eq. (18) then yields the values of  $x_{\min}$  presented in table I. Since  $A^2$  is a measure of the energy flux from the source and  $B^2$  the energy flux from the image, the reflection coefficient  $\mathfrak{R}$  for these longitudinal waves from the Earth's surface is then given by

$$\mathfrak{R} = B^2/A^2. \quad (19)$$

*Observation of the signal as a function of distance.* – The transmission station (Trio TR-9500) together with the ball antenna were installed at the northern end of a small street on the bank of river Rhein near Sennwald, Switzerland (Swiss chart number 1115 1:25000). The street between river Rhein and the nearby highway leads directly to the south. The transmitter as shown in fig. 4 was supplied by a 12 V car battery and the transmission itself was triggered by a 1 s oscillator to get not only the power signal but also a periodic quiet noise level at the receiver back end for calibration purposes. The receiver was composed of the receiving ball antenna, a low-noise gallium-arsenide field-effect-transistor amplifier (LNA-435) bought from SSB-electronics (Germany), a logarithmic radiofrequency detector AD8307 (Analog Devices) and a digital voltmeter (METEX-M3650) to read the power level of the transmitted signal. The output signal of the detector was also fed via an analog-to-digital converter (PICO-ADC10) to a personal computer. Every second the geographic coordinates of the GPS system (GARMIN 45) were fed to the laptop via a RS232 link in standard NMEA format. All components of the receiving equipment were supplied by another portable 12 V car battery. In the first couple of experiments the whole receiving equipment was carried by hand while during the later experiments a hand cart was used. All collected data were stored in an ASCII file which later on was transferred into an EXCEL sheet for further analysis.

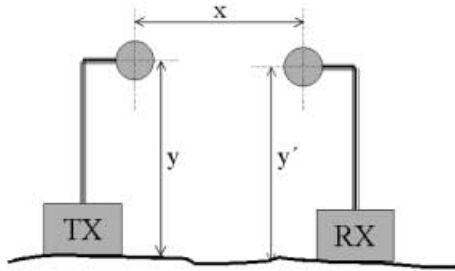


Fig. 4

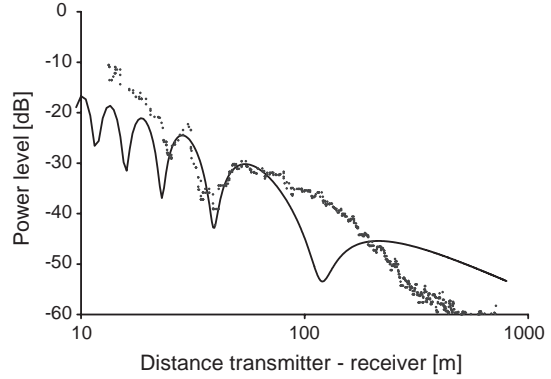


Fig. 5

Fig. 4 – Ultra-high-frequency transmitter (TX, left), portable receiving system (RX, right), both installed on the bank of river Rhein.

Fig. 5 – Received power (dB) as a function of distance  $x$ , where  $x$  was measured by a GPS system. The dots show one (V1) of 6 experiments; the solid line shows the values given by eq. (14).

*Comparison of theory with observation.* – Comparing the observations of the minima, as shown in fig. 5, the theoretically predicted positions of the minima,  $x_{\min}$ , as presented in table I, agree with the observations at  $x_{\min} = 39\text{m}$  and at  $23\text{m}$ . The other two minima probably exist, but the observations reveal nothing definite due to radiofrequency noise and measuring uncertainty in the GPS system in the order of  $\pm 5\text{m}$ . To compare the theory for the signal as a function of  $x$  it is first necessary to choose appropriate values for  $A$  and  $B$  to be used in eqs. (14) and (24). For a sufficient approximation the asymptotic approximation eq. (15) may be used for  $x = 40\text{m}$ . Neglecting the cosine term the mean observed value of the signal (relative to the value at  $x = 10\text{m}$ ) yields

$$(\omega k/2)(A^2 + B^2) = 1.0095 \tag{20}$$

and the observed (relative) minimum is

$$(\omega k/2)(A - B)^2 = 0.0637. \tag{21}$$

Solving eqs. (20) and (21) for  $A$  and  $B$  then yields

$$\sqrt{\omega k/2} \cdot A = 0.825 \quad \text{and} \quad \sqrt{\omega k/2} \cdot B = 0.573. \tag{22}$$

The theoretical graph for the signal, as given by eq. (14) using the values of  $A$  and  $B$  given by eqs. (22), is plotted in fig. 5 as a function of the distance  $x$ . The agreement between theory and the observations is quite satisfactory for  $x < 100\text{m}$ . The asymptotic approximation eq. (15) for  $A$  and  $B$  given by eqs. (22) becomes

$$\langle S_x \rangle_t = (1/x^2)[1 + 0.945 \cos k(R' - R)], \tag{23}$$

which also yields satisfactory agreement with the observations for  $20\text{m} < x < 100\text{m}$ . The reflection coefficient from eqs. (19) and (22) of the Earth's surface for these longitudinal waves is found to be

$$\Re = B^2/A^2 = 0.482. \tag{24}$$

The fact that reflection occurs is further proof that true waves are involved.

*Exponential loss of the signal with distance.* – It is apparent from fig. 5 that the observed signal beyond 100 m decreases more rapidly with distance than the inverse square of the distance. This loss corresponds to an additional exponential loss with distance corresponding to  $1/eth$  decrease in the signal for a distance of 145 m. This loss is probably due to the Ohmic losses produced by the currents induced in the Earth by the longitudinal  $\vec{E}$  field, which is parallel to the Earth's surface. No such loss would be expected for transverse wave, where the electric  $\vec{E}$  field is normal to the Earth's surface. This exponential decay of the signal with distance, thus, further indicates the fact that longitudinal electrodynamic waves are involved.

*Longitudinal electrodynamic waves can account for the huge signal observed from nuclear bomb explosions.* – One of us (Wesley) [5,6], was unable to explain the huge electrodynamic signal produced by a nuclear-bomb explosion, when it was assumed that only transverse electrodynamic waves are possible. It is now clear from the present demonstration of the actual existence of longitudinal waves, that the huge electrodynamic signal produced by a nuclear-bomb explosion is a longitudinal signal or wave. The electrons ejected radially outward produce a radial transient oscillating charge separation that readily generates a huge longitudinal electrodynamic signal. It may, thus, also be assumed that stellar novae and super novae will also be sources of extremely energetic transient longitudinal waves, that should be readily detectable on the Earth with the appropriate antenna to receive longitudinal waves.

\* \* \*

We thank H. BENZ for carrying and pulling the receiving equipment several times over distance of 1 kilometer as well as for contributing components and manufacturing the polarizer hardware. We thank also R. HASLER for looking after the transmitter station to prevent misuse and theft during the measurements. We especially thank F. AEBERSOLD for doing the special drawings and for manufacturing all aluminium balls on his milling machine. We also thank P. MESSMER for endless help and instructions concerning LaTeX- and MikTeX-related problems on my personal computer.

#### REFERENCES

- [1] JACKSON J. D., *Classical Electrodynamics* (John Wiley & Sons, New York) 1965, p. 180, eq. (6.37).
- [2] WESLEY J. P., *Proceedings of the 2nd Cologne Workshop Physics as a Science*, in *J. New Energy*, **5** (2001) 95.
- [3] WESLEY J. P., *Selected Topics in Scientific Physics* (Benjamin Wesley, Blumberg) 2001, pp. 125-127.
- [4] ROMIG H. R. *et al.*, *Reference Data For Radio Engineers*, edited by WESTMAN H. P., Vol. **6** (Howard W. Sams & Co., Inc.) 1982, pp. 28-3, Table (1).
- [5] WESLEY J. P., *Theory of electromagnetic field from a ground shot (nuclear bomb explosion)*, Univ. Calif. Rad. Lab Report-5177 (Livermore, California) 1958.
- [6] WESLEY J. P., *Theory of electromagnetic field from a high altitude shot (nuclear bomb explosion)*, Univ. Calif. Rad. Lab Report-5157 (Livermore, California) 1958.